THE JOURNAL OF COMPARATIVE NEUROLOGY 419:377–393 (2000)

Visual Cortical Projections and Chemoarchitecture of Macaque Monkey Pulvinar

MICHELLE M. ADAMS,[1,2] PATRICK R. HOF,[2–4] RICARDO GATTASS,[5] MAREE J. WEBSTER,[6] AND LESLIE G. UNGERLEIDER[1]*

[1]Laboratory of Brain and Cognition, National Institute of Mental Health, Bethesda, Maryland 20892

[2]Kastor Neurobiology of Aging Laboratory and Fishberg Research Center for Neurobiology Mount Sinai School of Medicine, New York, New York 10029

[3]Department of Geriatrics and Adult Development, Mount Sinai School of Medicine, New York, New York 10029

[4]Department of Ophthalmology, Mount Sinai School of Medicine, New York, New York 10029

[5]Departamento de Neurobiologia, Instituto de Biofísica Carlos Chagas Filho, Universidade Federal do Rio de Janeiro, Rio de Janeiro 21941-900, Brasil

[6]The Stanley Foundation Research Program, The Uniformed Services University for Health Sciences, Bethesda, Maryland 20814

ABSTRACT

We investigated the patterns of projections from the pulvinar to visual areas V1, V2, V4, and MT, and their relationships to pulvinar subdivisions based on patterns of calbindin (CB) immunostaining and estimates of visual field maps (P_1, P_2 and P_3). Multiple retrograde tracers were placed into V1, V2, V4, and/or MT in 11 adult macaque monkeys. The inferior pulvinar (PI) was subdivided into medial (PI_M), posterior (PI_P), central medial (PI_{CM}), and central lateral (PI_{CL}) regions, confirming earlier CB studies. The P_1 map includes PI_{CL} and the ventromedial portion of the lateral pulvinar (PL), P_2 is found in ventrolateral PL, and P_3 includes PI_P, PI_M, and PI_{CM}. Projections to areas V1 and V2 were found to be overlapping in P_1 and P_2, but those from P_2 to V2 were denser than those to V1. V2 also received light projections from PI_{CM} and, less reliably, from PI_M. Neurons projecting to V4 and MT were more abundant than those projecting to V1 and V2. Those projecting to V4 were observed in P_1, densely in P_2, and also in PI_{CM} and PI_P of P_3. Those projecting to MT were found in P_1–P_3, with the heaviest projection from P_3. Projections from P_3 to MT and V4 were mainly interdigitated, with the densest to MT arising from PI_M and the densest to V4 arising from PI_P and PI_{CM}. Because the calbindin-rich and -poor regions of P_3 corresponded to differential patterns of cortical connectivity, the results suggest that CB may further delineate functional subdivisions in the pulvinar. J. Comp. Neurol. 419:377–393, 2000. © 2000 Wiley-Liss, Inc.

Indexing terms: calcium-binding proteins; primate visual system; thalamocortical connections; visual thalamus

Over the course of evolution, there has been a disproportionate enlargement of the thalamus and of the association cortices (see Chalupa, 1991; Robinson and Petersen, 1992). A major contribution to this increase in the size of the thalamus is due to the pulvinar nucleus, a well-differentiated nucleus in the posterior thalamus (Olszewski, 1952; Jones, 1985). In the macaque monkey, the pulvinar is divided into four main cytoarchitectonic subdivisions: the inferior pulvinar (PI), the lateral pulvinar (PL), the medial pulvinar (PM), and the oral pulvinar (PO) (Olszewski, 1952).

Grant sponsor: American Health Assistance Foundation; Grant sponsor: the Brookdale Foundation; Grant sponsor: Pronex, CNPq, FAPERJ.

*Correspondence to: Dr. Leslie G. Ungerleider, Laboratory of Brain and Cognition, National Institute of Mental Health, Building 10, Room 4C104, 10 Center Drive MSC 1366, Bethesda, MD 20892-1366.
E-mail: lgu@ln.nimh.nih.gov

Received 25 August 1999; Revised 7 December 1999; Accepted 9 December 1999

© 2000 WILEY-LISS, INC.

Within the PI, PL, and PM subdivisions of the pulvinar, at least three separate visual fields have been described, but none corresponds precisely to the various cytoarchitectonic subdivisions. On the basis of electrophysiological mapping of the pulvinar, Bender (1981) described two separate fields, both of which are visuotopically organized. The first was termed the "PI" map; it is found mainly in rostrolateral PI, and extends into medial portions of adjacent PL. The second was termed the "PL" map; it partially surrounds the PI map and is located entirely in ventrolateral PL. Subsequently, Ungerleider et al. (1984) termed the PI and PL maps, respectively, the "P_1" and "P_2" fields of the pulvinar. A third field, P_3, was described by Ungerleider et al. (1984) based on connections with area MT. It is located posteromedially in PI, but also includes small ventral portions of PL and PM that lie dorsal to the brachium of the superior colliculus (see also Standage and Benevento, 1983). P_3 does not seem to have a well-defined retinotopic map, although it has yet to be mapped electrophysiologically. The locations of the P_1-P_3 fields relative to the cytoarchitectonic subdivisions of PI, PL, and PM are shown in Figure 1 (Table 1). Dorsal to the P_1-P_3 fields, near the boundary between PL and PM, lies a region termed "Pdm" (Petersen et al., 1985; Robinson et al., 1986). Like P_3, Pdm has little, if any, visuotopic organization.

Anatomic studies have shown that the P_1 and P_2 fields have connections with V1, V2, V4, and MT (Campos-Ortega and Hayhow, 1972; Benevento and Rezak, 1976; Ogren and Hendrickson, 1976; Benevento and Davis, 1977; Graham, 1982; Maunsell and Van Essen, 1983; Standage and Benevento, 1983; Ungerleider et al., 1983, 1984; Cusick et al., 1993; Gutierrez and Cusick, 1997), and both receive inputs from the superficial layers of the superior colliculus (Benevento and Fallon, 1975; Partlow et al., 1977; Harting et al., 1980; Benevento and Standage, 1983; Stepniewska et al., 1999). The P_3 field has connections with MT, MST, and FST (Maunsell and Van Essen, 1983; Standage and Benevento, 1983; Ungerleider et al., 1984; Boussaoud et al., 1992). Pdm also receives input from the superior colliculus (Benevento and Standage, 1983). Although its interconnections with the cortex are unknown, it contains neurons whose activity is related to visual spatial attention (Petersen et al., 1985; Robinson et al., 1986). Thus, these studies support the idea of separate functional fields in the pulvinar; however, they provide no way to relate these fields to cytoarchitectonic structure.

With respect to functional specialization in the thalamus, the distribution of certain calcium-binding proteins and other histochemical markers has been found to be particularly useful in defining patterns of regional specialization within many nuclei (Jones and Hendry, 1989; Hashikawa et al., 1991; Rausell and Jones, 1991). Recently, immunohistochemical techniques have been applied in an effort to understand better the organization of the pulvinar (Fig. 2). In the pulvinar nucleus of the squirrel and rhesus monkeys, Cusick and colleagues used an antibody to calbindin to redefine the organization of both PI and the ventral portion of PL (Cusick et al., 1993; Gutierrez et al., 1995; Gray et al., 1999). Most of the ventral portion of cytoarchitectonic PL, which appears as a moderately calbindin-immunoreactive area, was included in PI by the authors and termed the PI_L (lateral) subdivision. The most lateral portion of cytoarchitectonic PL was also included in PI and called $PI_{L\text{-}S}$, or the "shell" region ("S") of PI_L. Medially adjacent to PI_L, within what is cytoarchitectonically PI, lies a darkly stained area, which the authors termed the PI_C (central) subdivision of PI. Medial to PI_C is a calbindin-poor region, PI_M (medial), which they called the "calbindin-hole." Finally, the most medial subdivision, adjacent to PI_M, was termed PI_P (posterior), a triangular area bounded by PI_M, the brachium of the superior colliculus, and the dorsal portion of the medial geniculate complex. Thus, according to those authors, there are four subdivisions of PI, one of which, PI_L, is in the ventral portion of cytoarchitectonic PL, and two of which (PI_M and PI_C) extend above the brachium of the superior colliculus into cytoarchitectonic PM.

A somewhat comparable parcellation of the inferior pulvinar has been proposed by Stepniewska and Kaas (1997) (Fig. 2). Their scheme matched that of Cusick and colleagues for PI_P and PI_M (Cusick et al., 1993; Gutierrez et al., 1995). However, Stepniewska and Kaas (1997) did not consider the ventral portion of cytoarchitectonic PL to be part of the inferior pulvinar. Thus, they used the term PI_{CM} to refer to PI_C of Cusick and colleagues (i.e., the darkly stained area), and the term PI_{CL} to refer the most lateral portion of cytoarchitectonic PI.

The subdivisions of the pulvinar defined by calbindin immunoreactivity offers a new scheme that could be related to its functional organization. The present study was undertaken to relate the location of the V1-, V2-, V4-, and MT-projecting neurons to the pulvinar subdivisions defined by the distribution of calbindin. In addition, we tried to relate the distribution of cortical-projecting neurons to the three pulvinar fields, P_1, P_2, and P_3. In this study, we used the nomenclature of Stepniewska and Kaas (1997), which retains the original cytoarchitectonic border between PI and ventral PL. Preliminary data from the current study have been reported in abstract form (Adams et al., 1995).

MATERIALS AND METHODS

Eleven adult Rhesus monkeys (*Macaca mulatta*) were used in the present study. All experimental protocols were conducted within NIH guidelines for animal research and were approved by the Institutional Animal Care and Use Committee (IACUC) at both Mount Sinai School of Medicine and NIMH. In five animals, areas V1 and V2 were injected with one of two retrograde tracers, Fast Blue (FB; Sigma, St. Louis, MO) or Diamidino Yellow (DY; Sigma). In four animals, areas V4 and MT were injected with FB or DY. In an additional two cases, injections were made into areas V2, V4, and MT. These animals received Fluororuby (FR; Molecular Probes, Eugene, OR) in area V2, FB or DY in area V4, and DY or FB in area MT. Thus, there were a total of five injections in area V1, 7 in V2, 6 in V4, and 6 in MT (Table 2). All injections were intended to cover comparable visual field representations within these visual cortical areas.

Surgical procedures

Surgery was performed under aseptic conditions. Anesthesia was induced with ketamine hydrochloride (10 mg/kg, i.m.) and maintained with a mixture of isoflurane gas (1–2%) and oxygen to effect. Body temperature was maintained between 35°C and 37°C by heating pads (circulat-

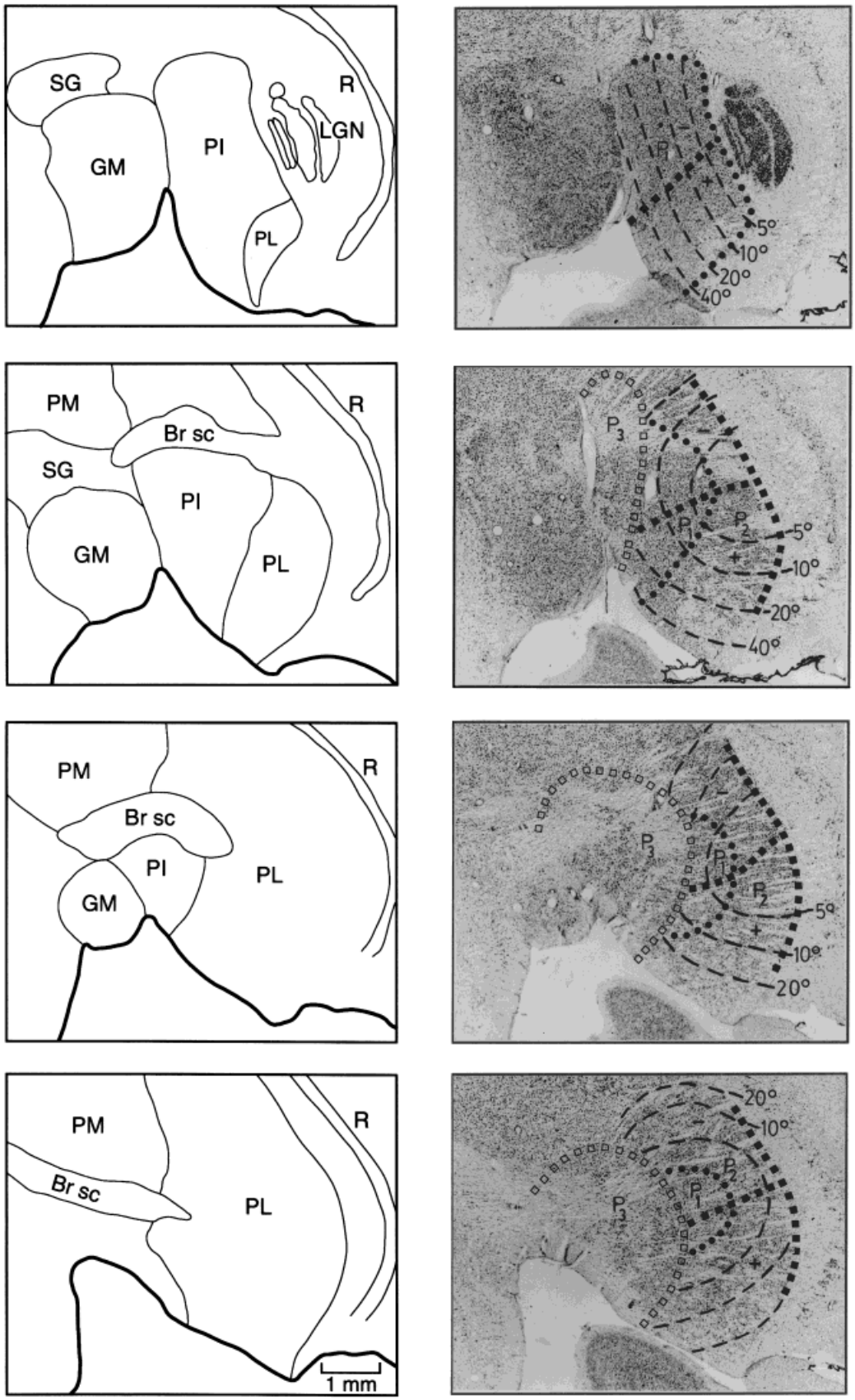

Fig. 1. Representative coronal sections stained for Nissl through the rostral (top)-to-caudal (bottom) extent of the pulvinar. **Left:** cytoarchitectonic subdivisions, according to Olszewski (1952). **Right:** the pulvinar fields, P_1, P_2, and P_3, are shown superimposed on each section. Solid circles indicate the representation of the vertical meridian, solid squares indicate the representation of the horizontal meridian, dashes indicate isoeccentricity lines, and open squares indicate the border of P_3. The plus sign indicates the upper visual field representation and the minus sign the lower field representation. The sections are spaced 0.5 mm apart. For abbreviations, see Table 1. Scale bar = 1 mm in lower left panel (applies to all frames).

ing warm water) surrounding the animal, and heart and respiratory rates were monitored throughout the surgery. A midline incision and unilateral craniotomy was performed in all animals. After the craniotomy, the dura was opened to expose the areas of interest. Pressure injections were made with a 1-μl Hamilton syringe with a beveled 27-gauge needle, which was guided into the appropriate site with the aid of an operating microscope. Up to 22 injections (0.2 μl each at each site) of 4% aqueous solutions of FB, DY, or FR were placed in a given area in the cortex. Sulcal and gyral landmarks were used to identify the location of areas V1, V2, V4, and MT (Daniel and Whitteridge, 1961; Zeki, 1974; Ungerleider and Mishkin, 1979; Gattass and Gross, 1981; Van Essen et al., 1981; Gattass et al., 1981, 1988; Ungerleider and Desimone, 1986).

TABLE 1. Abbreviations of Thalamic Nuclei and Cortical Sulci

Subcortical regions		Cortical sulci	
Br sc	Brachium of the superior colliculus	io	Inferior occipital sulcus
GM	Medial geniculate nucleus	ip	Intraparietal sulcus
LGN	Lateral geniculate nucleus	la	Lateral sulcus
PI	Inferior pulvinar	lu	Lunate sulcus
PI_{CL}	Inferior pulvinar, central lateral subdivision	st	Superior temporal sulcus
PI_{CM}	Inferior pulvinar, central medial subdivision		
PI_{L}	Inferior pulvinar, lateral subdivision		
$PI_{L\text{-}S}$	Inferior pulvinar, lateral shell subdivision ("S")		
PI_{M}	Inferior pulvinar, medial subdivision		
PI_{P}	Inferior pulvinar, posterior subdivision		
PL	Lateral pulvinar		
PL_{VL}	Ventrolateral PL		
PL_{VM}	Ventromedial PL		
PM	Medial pulvinar		
R	Reticular nucleus		
SG	Suprageniculate nucleus		

Injections in area V1 were placed in a vertical strip of opercular cortex parallel to the V1/V2 border approximately 5 mm posterior to the lunate sulcus. This region composes the foveal and parafoveal portions of the contralateral lower visual hemifield close to the vertical meridian. Injections in area V2 were placed in a strip of cortex parallel to the V1 injections along the posterior margin of the lunate sulcus, with special care to avoid spread of the dye in the subcortical white matter beneath area V2. Thus, the V1 and V2 injections were in retinotopic register. For area V4, injections were placed along a descending line starting at the level of the bifurcation of the superior temporal sulcus, thus avoiding the dorsal prelunate area (DP). The V4 injection extended in a vertical strip for approximately 10 mm, approximately to the level of the inferior occipital sulcus. Thus, as in areas V1 and V2, the injections in area V4 included foveal and parafoveal representations in the contralateral lower visual field. This portion of macaque V4 likely corresponds to squirrel monkey DL_c (Cusick and Kaas, 1988).

In four of the six monkeys with injections into area MT, the intention was to inject as much of MT as possible. Accordingly, in these four monkeys, the cortex of the dorsal bank of the posterior portion of the superior temporal sulcus was surgically aspirated, and tracer injections were then placed in the floor of the sulcus, presumably affecting both the upper and lower visual field representations. For the remaining two monkeys with MT injections, the injection sites were located by electrophysiological mapping techniques (Desimone and Ungerleider, 1986). After a desired injection site was identified, a guide tube was advanced through the dura and placed 300 μm above the intended site. A microelectrode was then advanced

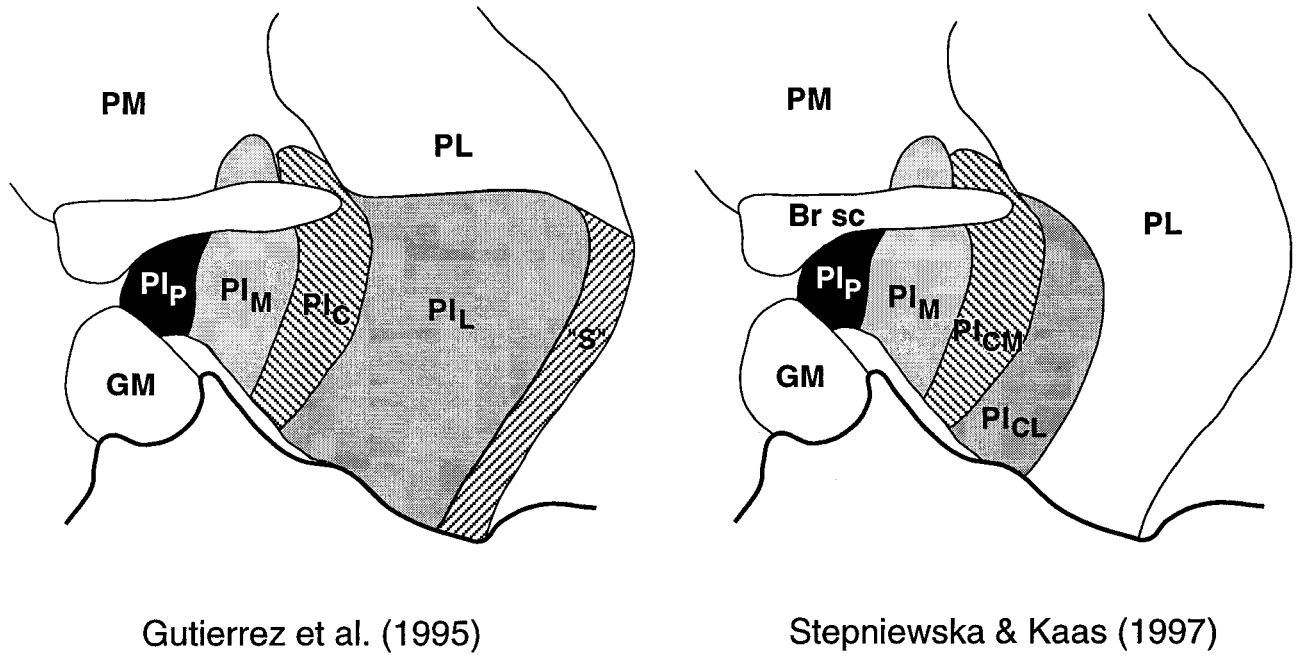

Fig. 2. Schematic drawings of the macaque pulvinar showing alternative subdivisions, as defined by calbindin immunohistochemistry. **Left:** subdivisions proposed by Gutierrez et al. (1995). "S" is the lateral shell subdivision of PI. © 1995 Wiley-Liss, Inc. Adapted by permission of Wiley-Liss, Inc. **Right:** subdivisions proposed by Stepniewska and Kaas (1997). Modified from Stepniewska and Kaas (1997). Reprinted with permission of Cambridge University Press. For abbreviations, see Table 1.

TABLE 2. Location of Retrogradely Labeled Cells in the Chemoarchitectonic Subdivisions of the P_1, P_2, and P_3 Visual Field Maps of the Pulvinar[1]

	P_1		P_2	P_3		
Location	PI_{CL}	PL_{VM}	PL_{VL}	PI_P	PI_M	PI_{CM}
V1 injection						
Case RH1	+	−	+	−	−	−
Case RH2	+	+	+	−	−	−
Case RH3	+	−	+	−	−	−
Case RH4	+	+	+	−	−	−
Case RH5	+	−	+	−	−	−
V2 injection						
Case RH1	+	−	+	−	−	+
Case RH2	+	+	+	−	−	+
Case RH3	+	+	+	−	+	+
Case RH4	+	+	+	−	+	+
Case RH5	+	+	+	−	−	+
Case RH6	+	+	+	−	+	+
Case RH7	+	−	+	−	−	+
V4 injection						
Case RH6	+	+	+	+	−	+
Case RH7	+	+	+	+	−	+
Case RH8	+	+	+	+	−	+
Case RH9	+	+	+	+	−	+
Case RH10	+	+	+	+	−	+
Case RH11	+	+	+	+	−	+
MT injections						
Case RH6	+	+	+	+	+	+
Case RH7	+	+	+	+	+	+
Case RH8	+	+	+	+	+	+
Case RH9	+	−	+	+	+	+
Case RH10[2]	+	+	+	+	+	+
Case RH11[2]	+	+	+	+	+	+

[1]Cells projecting to area V2 occupied the same areas as those projecting to area V1, namely, the P_1 and P_2 fields. PI_{CM} and PI_M of P_3 had retrogradely labeled cells projecting to area V2. Cells projecting to areas V4 and MT were found within P_1–P_3, with the densest projections to V4 from P_1 and P_2, and to MT from the PI_M portion of P_3. For abbreviations, see Table 1.
[2]Animals with MT injections that were prepared under physiologic guidance.

through the guide tube and the visuotopic location of the injection site was confirmed. The electrode was then withdrawn from the guide tube and replaced by a 1-μl Hamilton syringe. To minimize leakage of the tracer into the electrode track, the syringe was left in place 20 minutes after injections. In these two cases, the intention was to inject only the lower visual field representation of MT. All of the injections were verified anatomically.

Histologic processing

After surgery, a survival time of 21 days was set to allow for reliable retrograde transport of FB, DY, and FR (Campbell et al., 1991; Hof et al., 1995). Then, the animals were perfused as previously described (Hof and Nimchinsky, 1992; Hof and Morrison, 1995; Hof et al., 1995). Briefly, the animals were deeply anesthetized with ketamine hydrochloride (25 mg/kg i.m.) and pentobarbital sodium (20–35 mg/kg i.v., as necessary), intubated and mechanically ventilated. The chest was then opened, the heart exposed, and 1.5 ml of 0.1% sodium nitrite was injected into the left ventricle. The descending aorta was clamped and the monkeys were perfused transcardially with cold 1% paraformaldehyde in phosphate buffer (pH 7.4) for 1 minute followed by cold 4% paraformaldehyde for 10–12 minutes. The brains were then removed from the skull, cut into 2-cm coronal blocks, and postfixed for 6 hours. The blocks were cryoprotected in a series of graded sucrose solutions (12, 16, 18, and 30%) in phosphate-buffered saline (PBS; pH 7.4), and subsequently immersed into a 2-methyl-butane (95%) solution at −70°C and maintained at this temperature until sectioned (Rosene et al., 1986). Frozen sections, 40 μm thick, were cut from the coronal blocks on a sliding microtome. Sections were mounted every 500 μm onto gelatin-coated slides for analysis of the retrogradely labeled cells. Adjacent series of sections were stained for Nissl or were processed for calbindin immunohistochemistry. The remaining sections were cryoprotected and stored in serial order at −20°C.

For immunohistochemistry, free-floating sections were incubated for 48 hours at 4°C with the monoclonal antibody against the calcium-binding protein calbindin (Swant, Bellinzona, Switzerland; Celio et al., 1990), at a dilution of 1:5,000 in PBS containing 0.3% Triton X-100 and 0.5 mg/ml bovine serum albumin. The sections were then processed with the avidin-biotin method by using a Vectastain ABC kit (Vector Laboratories, Burlingame, CA) and 3,3′-diaminobenzidine as a chromogen. Calbindin immunoreactivity was subsequently intensified in 0.005% osmium tetroxide.

Data analysis

Each labeled neuron was charted at 100× magnification by using a computerized plotting system consisting of a Zeiss Axioplan microscope equipped with XY-position encoders attached to a microscope stage (Minnesota Datametrics). The data from these chartings were then overlaid onto a photograph of the adjacent section stained for calbindin immunohistochemistry to observe the location of the retrogradely labeled cells in relation to the chemoarchitectonic subdivisions of the pulvinar. Calbindin-stained sections were compared with those stained for Nissl to relate chemoarchitectonic subdivisions to those based on cytoarchitecture.

The visual field representations of the injection sites were estimated based on previously published mapping studies of V1, V2, V4, and MT (Daniel and Whitteridge, 1961; Gattass and Gross, 1981; Gattass et al., 1981, 1988). The P_1 and P_2 retinotopic maps in the pulvinar were charted onto Nissl- and calbindin-stained sections based on previously published work by Bender (1981) and Ungerleider et al. (1983, 1984). The P_3 map was similarly charted. The first estimate of the P_3 border was guided by

Ungerleider et al. (1984) and then by the distribution of label in the current MT cases. The dorsal border of P_3 (i.e., the portion above the brachium of the superior colliculus) was adjusted to be compatible with the distribution of calbindin immunoreactivity. Thus, our assignment of cells to P_1-P_3 is based on estimated borders of these regions.

RESULTS

In the following sections, we first describe the chemoarchitectonic subdivisions of the pulvinar based on the distribution of calbindin immunohistochemistry, and then relate these subdivisions to the visual field maps, P_1-P_3, as described in earlier studies (Bender, 1981; Ungerleider et al., 1983, 1984). We then relate the connectional patterns of V1, V2, V4, and MT with these visual field maps. Finally, we relate the distribution of calbindin staining to the patterns of connections.

Chemoarchitectonic subdivisions and projection fields of the pulvinar

As shown in Figure 3, calbindin immunoreactivity clearly revealed the four subdivisions of PI described previously by Stepniewska and Kaas (1997). At rostral levels of cytoarchitectonic PI, where the LGN was present, a single PI subdivision, PI_{CL}, was seen. Additionally, at these rostral levels, small portions of ventral PL were visible ventrolateral to PI_{CL}. As one proceeded to more caudal levels of the inferior pulvinar, PI_{CL} became progressively smaller and PI_M and PI_{CM} appeared. At the most caudal levels of cytoarchitectonic PI, the four distinct subdivisions of PI were evident. From medial to lateral these included, PI_P, PI_M, PI_{CM}, and PI_{CL}.

Figure 4 illustrates the distribution of calbindin-immunoreactive neurons and neuropil staining within the chemoarchitectonic subdivisions of the pulvinar. Both the PI_P and PI_{CM} subdivisions had the heaviest calbindin immunoreactivity, with many darkly stained small cells and dense neuropil. The difference between the two subdivisions was that PI_{CM} contained a few large cells (not shown in figure), which were absent in PI_P. The PI_M subdivision, the "calbindin-hole" of cytoarchitectonic PI, located between PI_P and PI_{CM}, contained light neuropil staining but many calbindin-containing neurons. The PI_{CL} subdivision had moderate calbindin staining. Within this zone, there was a dense population of small calbindin-containing neurons and moderate neuropil staining, as well as a small number of large neurons. The small calbindin-containing neurons had a moderately stained soma with a few lightly stained dendrites, whereas the larger immunoreactive neurons had a darkly stained soma with dark radiating dendrites. On the whole, PI_{CL} had denser neuropil staining and more darkly stained calbindin-immunoreactive neurons compared with PI_M, but the staining was not as intense as in PI_P and PI_{CM}. The distinguishing feature of PI_{CL} was the numerous large cells that were scattered throughout this subdivision.

The ventral portion of cytoarchitectonic PL was similar to PI_{CL}, in that both of these regions had a large number of small calbindin-containing neurons and a few scattered large cells. Although Cusick et al. (1993) and Gutierrez et al. (1995) considered this subdivision as part of PI_{CL} (PI_L in their terminology), PI_{CL} and ventral PL could be distinguished by the presence of horizontally oriented fiber bundles in the latter. Dorsally in the pulvinar, cytoarchitectonic PM also contained many small calbindin-immunoreactive neurons and a few scattered large neurons (not shown in figure). However, in PM the neuropil was more intensely stained than in PL.

As previously described by Ungerleider et al. (1984), the P_1 field is found mainly in ventrolateral PI, and extends into portions of adjacent ventromedial PL. The P_2 field partially surrounds the P_1 field and is located entirely in ventrolateral PL, and the P_3 field is found in PI, but also includes small ventral portions of PL and PM that lie dorsal to the brachium of the superior colliculus. Based on the patterns of calbindin immunohistochemistry, P_1 includes PI_{CL} and the ventromedial portion of PL (PL_{VM}), P_2 includes the ventrolateral portion of PL (PL_{VL}), and P_3 contains the PI_P, PI_M, and PI_{CM} subdivisions of PI. Therefore, the calbindin immunostaining can be used as marker for P_3, but not for the border between P_1 and P_2. The relationship between the chemoarchitectonic subdivisions of the pulvinar and the P_1-P_3 maps are illustrated for individual cases in Figures 5–8.

Projections to V1, V2, V4, and MT from P_1, P_2, and P_3

Area V1. In five monkeys, FB or DY was injected in the lower visual field representation of area V1 at approximately 3–10 degrees eccentricity, close to the vertical meridian. The pattern of retrogradely labeled neurons showed projections from both P_1 and P_2 at the appropriate visuotopic locations, as shown in Figures 5 and 6. In all cases, the neurons in P_1 were mainly contained in the PI_{CL} zone, with some additional neurons within the immediately adjacent ventromedial PL (Fig. 6). The neurons in P_2 were as numerous as in P_1, but were more widely distributed in P_2, as would be expected by the enlarged representation of the visual field in P_2 relative to the map in P_1. No retrogradely labeled cells were observed within P_3 (see Table 2).

Area V2. In the same five monkeys, FB or DY was injected in area V2 parallel to the V1 injection at similar eccentricities, but in most cases the V2 injection covered a somewhat larger portion of the visual field representation (Figs. 5, 6). In two additional monkeys (cases RH6 and RH7), the same region of V2 was injected, but V1 was not. In all V2 cases, retrogradely neurons were found in P_1 and P_2 (see Table 2). Like the projections to area V1, the neurons projecting to area V2 from P_1 and P_2 were in topographic register with the visual field maps (Figs. 5, 6). In case RH1, the P_1 neurons were located exclusively in PI_{CL}, but in the other five V2 cases, P_1 neurons seemed to extend from PI_{CL} into adjacent ventromedial PL (Fig. 5). In case RH2, the cells in P_1 and P_2 seemed to merge into a single region (Fig. 6). This finding was due to the fact that the V1 and V2 injections in this case likely included the representation of the vertical meridian and, therefore, labeling was present at the P_1/P_2 border where this meridian is represented. Also, it should be noted that the injection in RH1 likely crossed the representation of the horizontal meridian; thus, the labeled neurons included portions of the upper visual field in P_1 and P_2, as well as the lower field. In four of the five monkeys with V1 and V2 injections, a few double-labeled neurons were observed in P_2.

In all V2 cases, unlike in the V1 cases, there were retrogradely labeled neurons in a third zone that fell

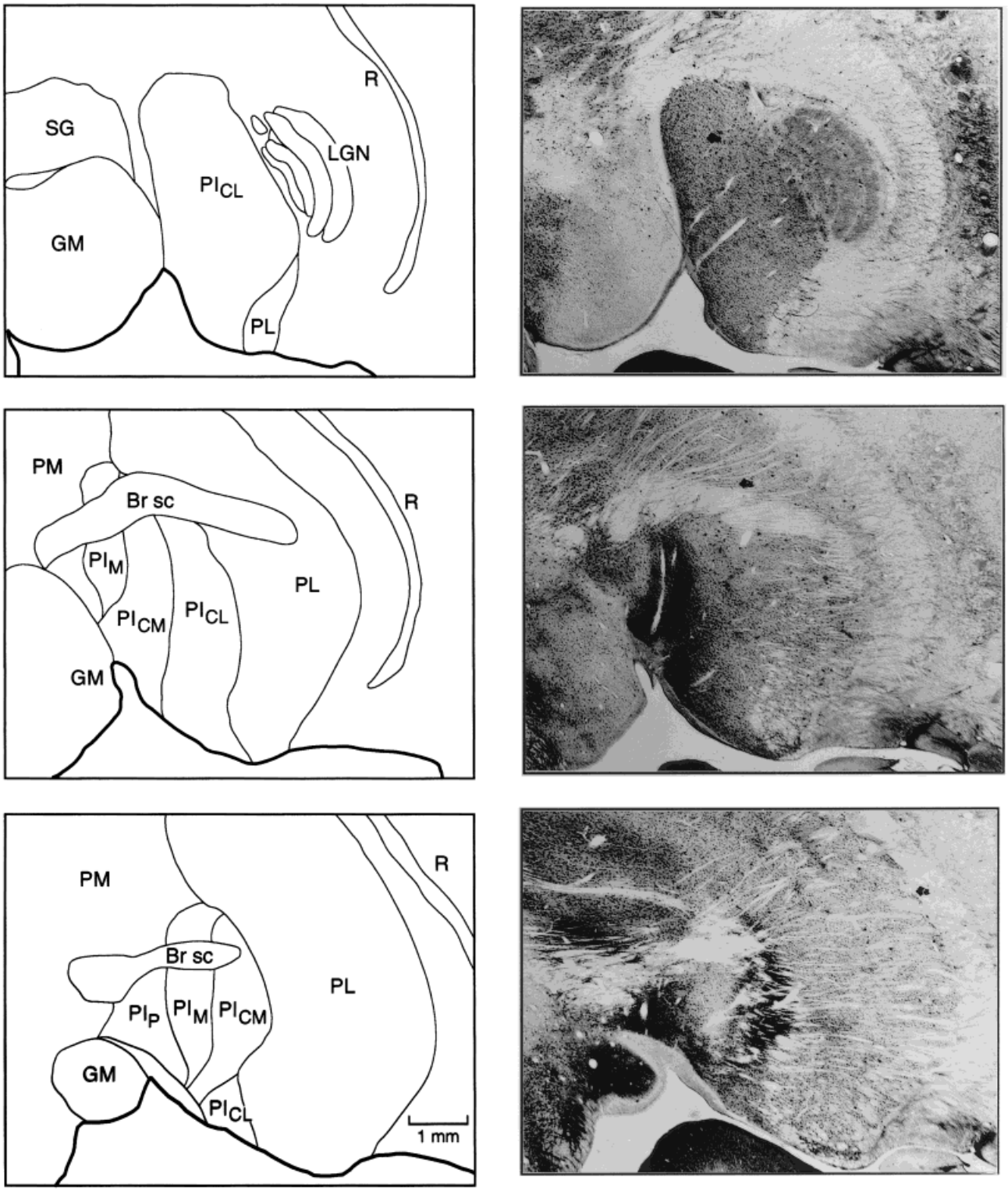

Fig. 3. **Right:** representative photomicrographs of sections processed for calbindin immunohistochemistry through the rostral (top)-to-caudal (bottom) extent of the pulvinar. These sections show four distinct chemoarchitectonic subdivisions of cytoarchitectonic PI, whose borders are shown in the line drawings (**left**). For abbreviations, see Table 1. Scale bar = 1 mm in lower left panel (applies to all panels).

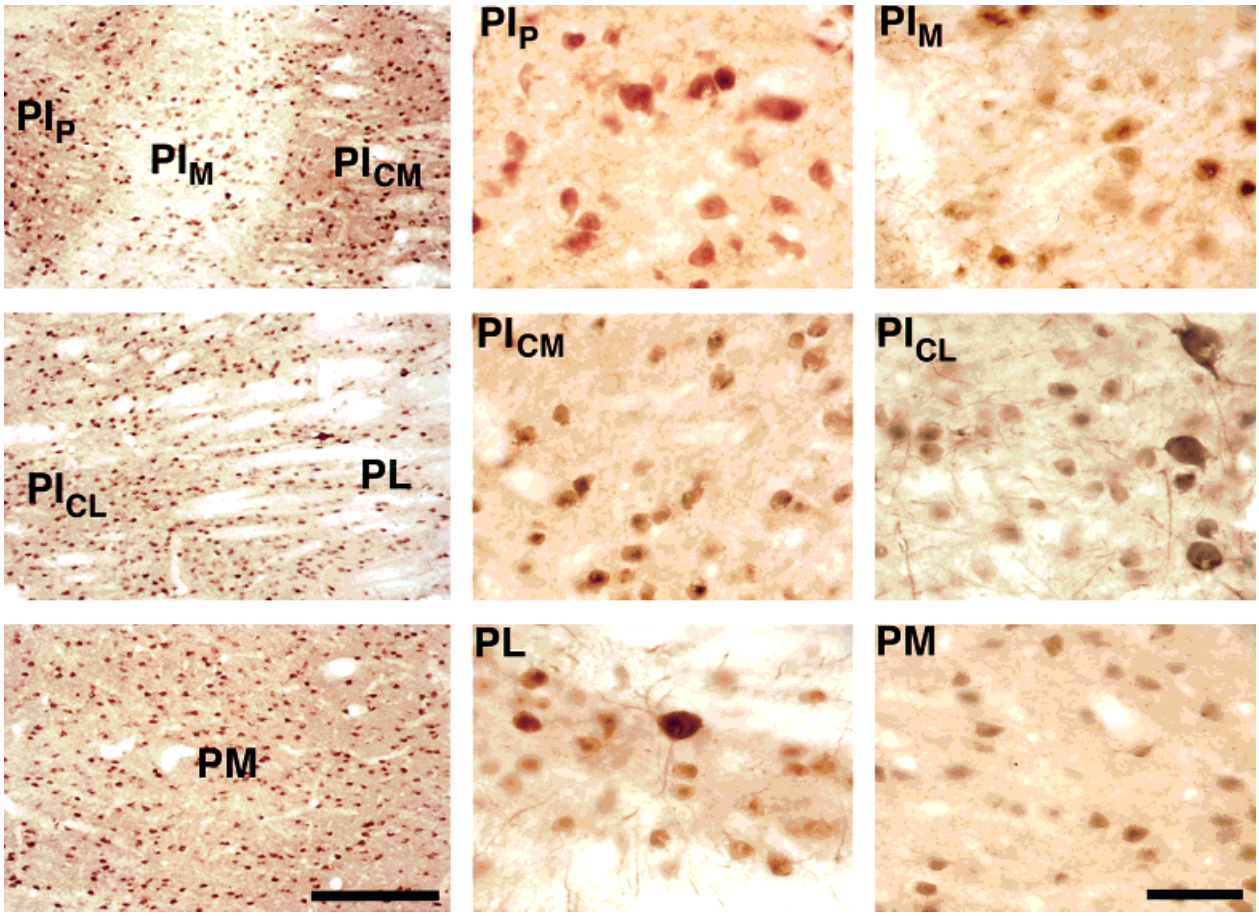

Fig. 4. The distribution of calbindin-positive neurons and neuropil staining within the chemoarchitectonic subdivisions of the pulvinar. Each region labeled in the panels of the column on the left is shown at higher magnification in the panels of the two columns on the right. For abbreviations, see Table 1. Scale bar = 200 μm in lower left panel (applies to all panels in the left column), 30 μm in the lower right panel (applies to all panels in the middle and right columns).

within the P_3 field. Within P_3, neurons were found in PI_{CM} in all cases, and also in PI_M in three of the seven cases. The projection from PI_{CM} to area V2 was not as dense as that from P_1 and P_2 but was heavier that that from PI_M. In no case were labeled neurons seen in PI_P (Table 2).

Area V4. In the six monkeys with injections into area V4, FB or DY was placed into the lower visual field representation of the area, at approximately 2–10 degrees eccentricity (Gattass et al., 1988). There were projections from P_1, P_2 and P_3 in every case (Table 2). The most extensive projection zone was from P_2, with sparser projections from P_1 and still sparser from P_3 (Figs. 7, 8). The locations of labeled neurons in P_1 and P_2 were in good agreement with their visual field maps. In all cases, the neurons projecting from P_1 were found in both the PI_{CL} and adjacent ventromedial PL regions. Those projecting from P_3 were observed in PI_P and PI_{CM} but not in PI_M, which was devoid of label. In the two cases with injections of V2 and V4 (RH6 and RH7), no double-labeled cells were seen.

Area MT. In the same six animals with V4 injections, FB or DY was placed into area MT. Two were placed under physiological control and four were made under visual inspection after exposing the region through surgical aspiration of the upper bank of the caudal superior temporal sulcus. In the four monkeys prepared under visual inspection, the intention was to fill the entire extent of the region to ensure that the visual field representation included in the MT injection overlapped the area that was included in the V4 injection, namely, the representation of the lower visual field. In these cases, there was contamination of FST (Boussaoud et al., 1990) in the injection site, but not of V4t (Desimone and Ungerleider, 1986). In the two animals injected under physiological control, injections were placed in the lower visual field representation of MT. After injections into MT, retrogradely labeled neurons were found sparsely in P_1 and P_2, and densely in P_3, as illustrated in Figures 7 and 8. In all cases, retrogradely labeled neurons were seen in the PI_{CL} subdivision of P_1, and in five of the six cases, labeled neurons were found in the ventromedial portion of the PL region of P_1 as well. All cases showed label in P_2. Although the labeling was sparse in both P_1 and P_2, it covered a large portion of these maps, consistent with the large extent of the visual field representation included in the MT injections. In all of the monkeys with MT injections, PI_P, PI_M, and PI_{CM} of P_3 contained labeled neurons (see Table 2). The densest projection was from PI_M, and this projection extended above the brachium of the superior colliculus, as shown in Figures

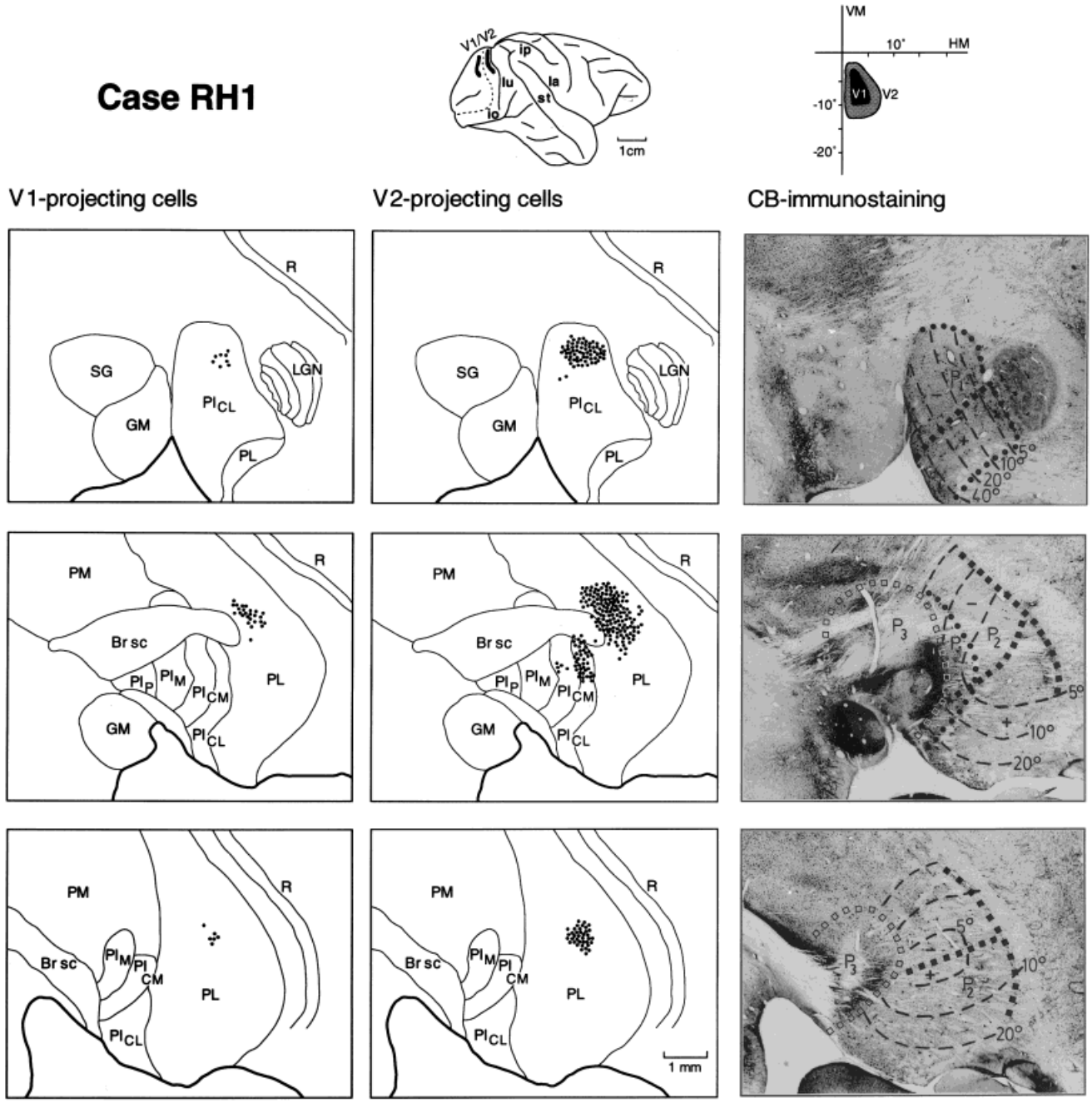

Fig. 5. Case RH1: Distribution of retrogradely labeled neurons in the pulvinar after injections of Diamidino Yellow in area V1 and Fast Blue in area V2. The injection sites are shown on a lateral view of the right hemisphere at the top middle. Dashed lines indicate the V1/V2 border. The estimated visual field representation of these injection sites is shown at top right. The labeled cells (black dots) are shown on a rostral (top) -to-caudal (bottom) series of coronal sections throughout the pulvinar. The retrogradely labeled cells seen after the injection in area V1 are in the left column and those seen after the injection in area V2 are in the middle column. The right column shows the photomicrographs of calbindin immunohistochemistry with the visual field representations within P_1 and P_2, and the border of P_3 superimposed on the sections. CB, calbindin; HM, horizontal meridian; VM, vertical meridian. For other abbreviations, see Table 1. Scale bar = 1 mm in lower middle panel (applies to all frames).

7 and 8. The projection from PI_P and PI_{CM} was less dense, but heavier than that from P_1 and P_2. In four of the six monkeys, a few double-labeled neurons projecting to MT and V4 were seen in PI_{CM} and PI_{CL}. There were no double-labeled neurons projecting to areas MT and V2.

Relationship between chemoarchitectonic subdivisions and patterns of projections

The P_1 and P_2 fields. Neurons in both P_1 and P_2 were found to project to V1 and V2. The neurons in

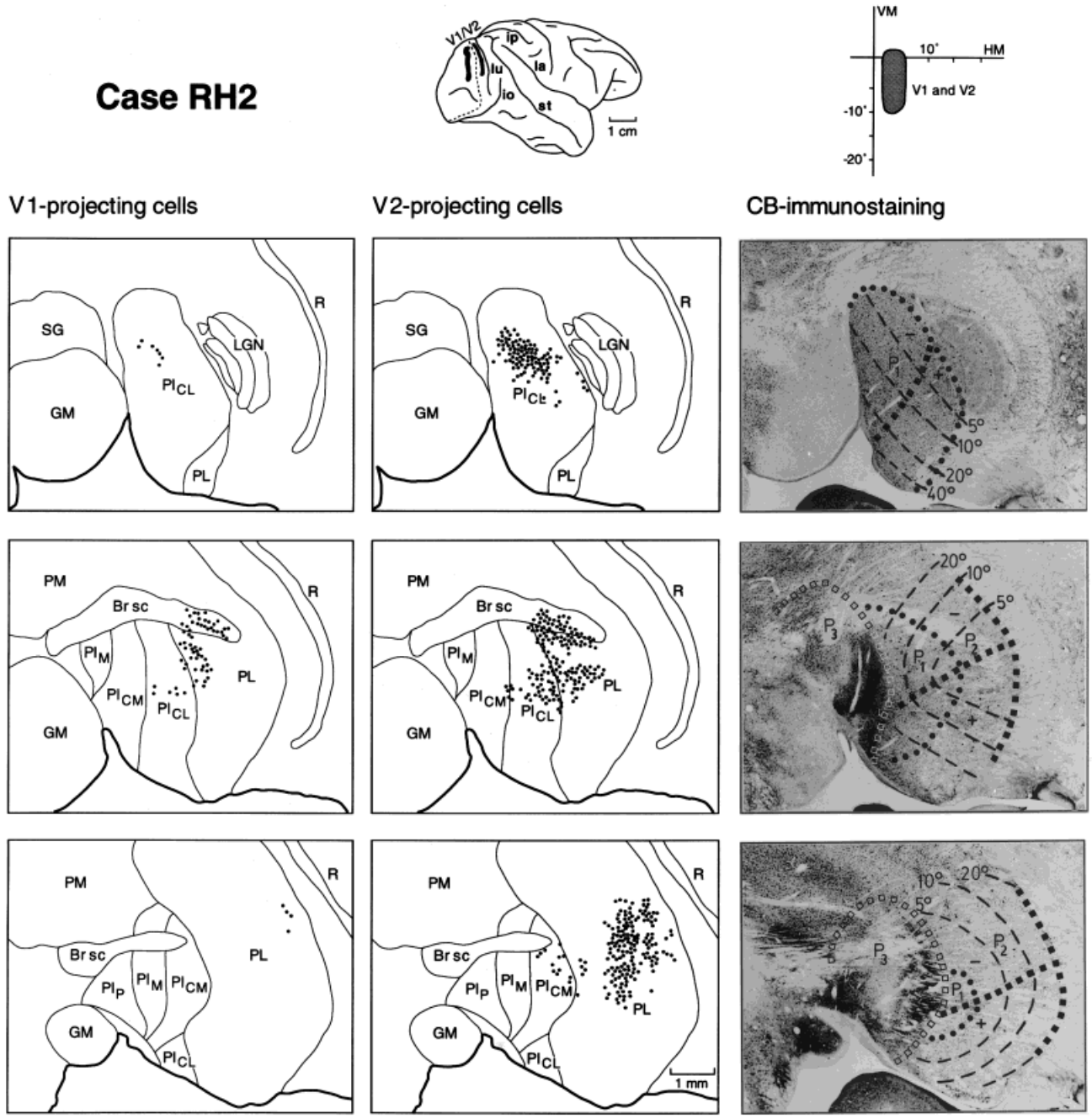

Fig. 6. Case RH2. Distribution of retrogradely labeled neurons in the pulvinar after injections of Fast Blue in area V1 and Diamidino Yellow in area V2. For all conventions, see Figure 5. Scale bar = 1 mm in lower middle panel (applies to all frames).

these fields that projected to V2 overlapped those projecting to V1 in all monkeys (Figs. 5, 6). In both P_1 and P_2, a few double-labeled neurons were observed projecting to V1 and V2. In the two animals with injections in areas V2, V4, and MT, the neurons projecting to area V2 overlapped more extensively with those projecting to area V4 than with those projecting to area MT (Fig. 8). The most extensive region of overlap of cells projecting to areas V2 and V4 occurred in PI_{CL} of P_1 and ventrolateral PL of P_2. Because the projections from P_1 and P_2 to MT were sparse, there was minimal overlap with those projecting to V2.

The P_3 field. The retrogradely labeled neurons located in P_3 were found to project to areas V2, V4, and MT, but not to V1. Each chemoarchitectonic region within P_3 was observed to project differentially to these cortical areas. In all seven cases, projections to V2 arose from PI_{CM}, and in three of these cases retrogradely

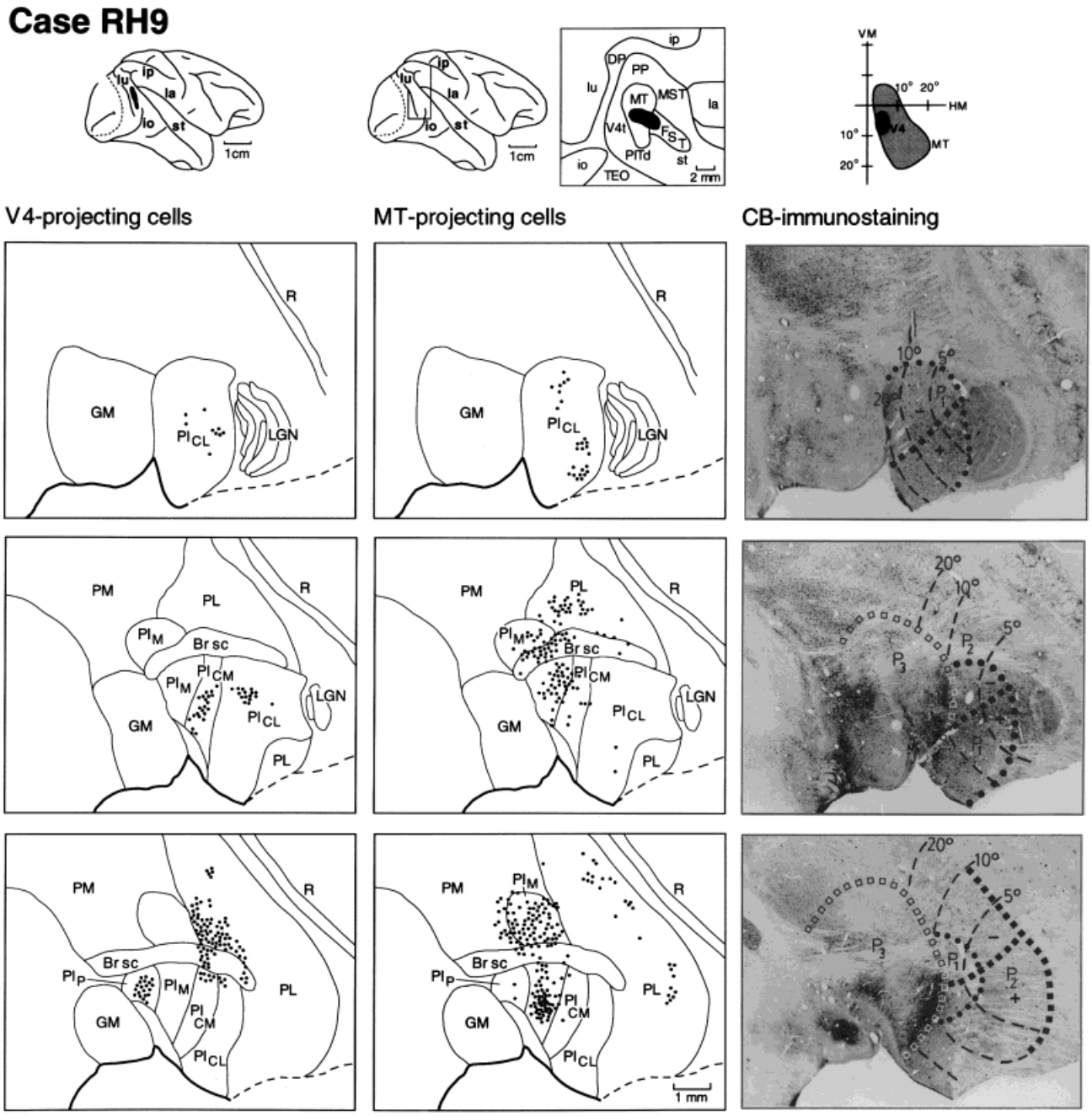

Fig. 7. Case RH9. Distribution of retrogradely labeled neurons in the pulvinar after injections of Diamidino Yellow in area MT and Fast Blue in area V4. The injection in area V4 is shown on a lateral view of the hemisphere at top left. The injection in area MT is shown on a flattened map of the caudal portion of the superior temporal sulcus and surrounding cortex; the portion of the flattened sulcus is indicated on lateral view of the brain at top middle. The estimated visual field representations of these injection sites are shown on top right. The retrogradely labeled cells seen after the area V4 injection are in the left column and those seen after the area MT injection are in the middle column. Dashed lines at the base of the pulvinar indicate torn tissue. The right column shows photomicrographs of calbindin immunohistochemistry with the visual field representations within P_1 and P_2 and the border of P_3 superimposed on the sections. DP, dorsal prelunate area; FST, fundus of the superior temporal area; MST, medial superior temporal area; PITd, posterior inferior temporal area, dorsal part; PP, posterior parietal area; TEO, inferior temporal area bordering occipital cortex. For all other conventions, see Figure 5. Scale bar = 1 mm in lower middle panel (applies to all frames).

labeled cells were also seen in PI_M. Projections to area V4 arose from PI_P and PI_{CM} in all cases, but none arose from PI_M. Area MT received projections from all subdivisions of P_3, with the densest projection arising from PI_M. In the two monkeys injected in areas V2, V4, and MT, there were dense overlapping projection zones of

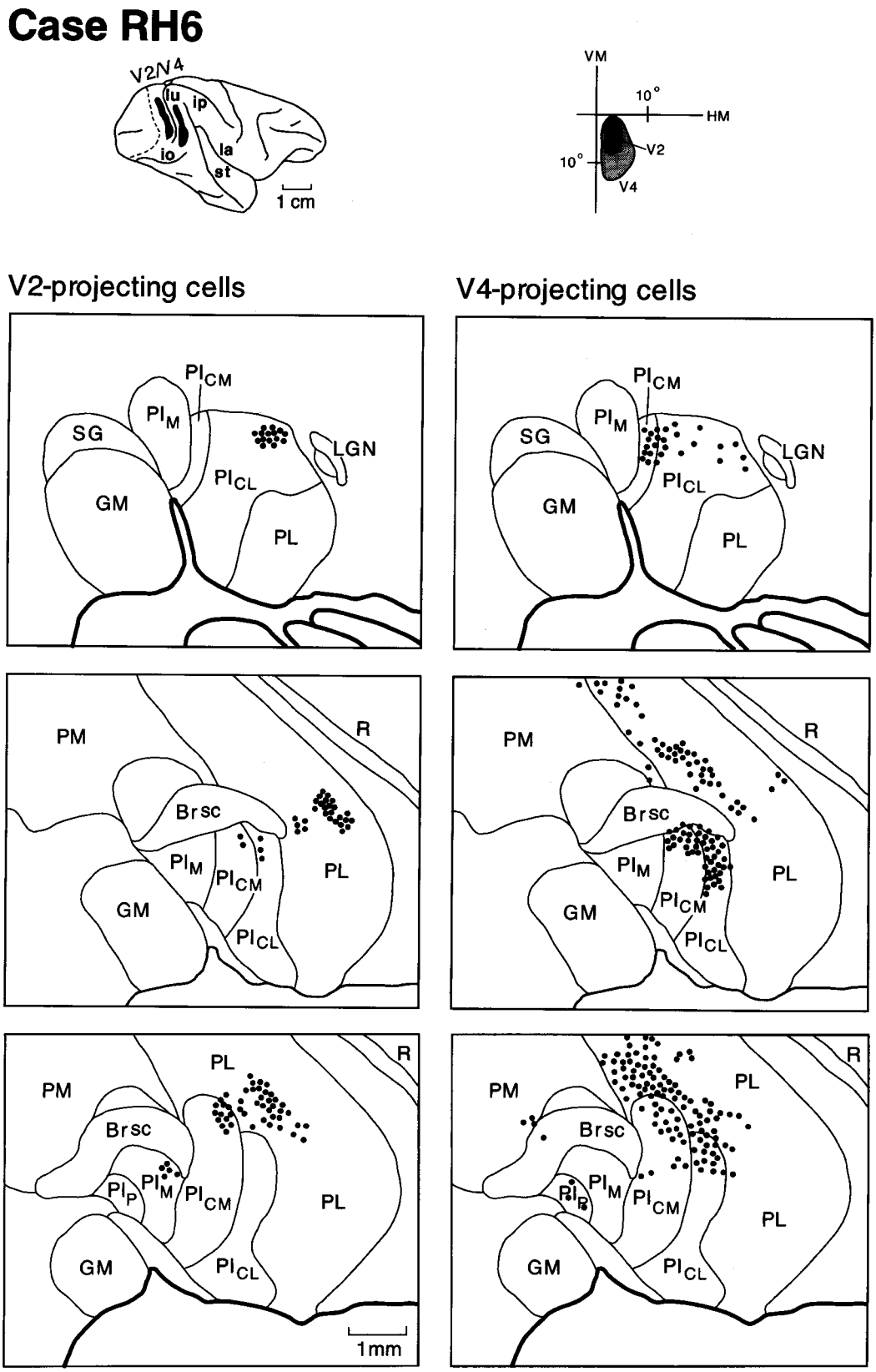

Fig. 8. Case RH6: Distribution of retrogradely labeled neurons in the pulvinar after injections of Fluororuby in area V2, Diamidino Yellow in area V4, and Fast Blue in area MT. The injections into areas V4 and V2 are shown on a lateral view of the hemisphere at the top left. The injection in area MT is shown on a flattened map of the caudal portion of the superior temporal sulcus and surrounding cortex; the portion of the flattened sulcus is indicated on the lateral view of the brain at top right. The estimated visual field representations of these injection sites are also shown at top. The retrogradely labeled cells seen after the injection in area V2 are in the left column of the left facing page, those seen after the injection in area V4 are in the right column of the left facing page, and those seen after the injection in area MT are in the left column of the right facing page. For all other conventions, see Figures 5 and 7. Scale bar = 1 mm in lower left panel on left facing page (applies to all frames).

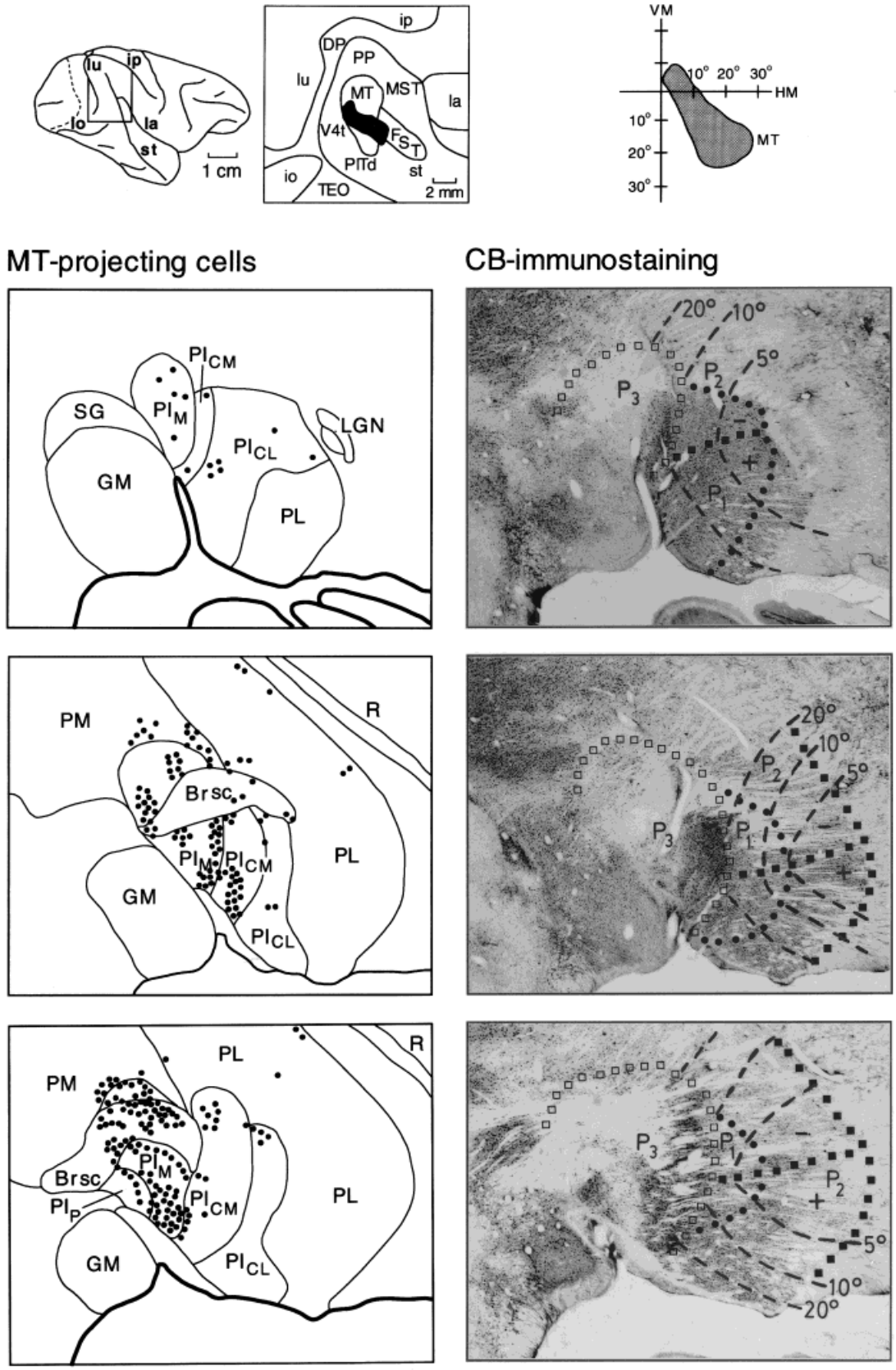

Figure 8 (Continued)

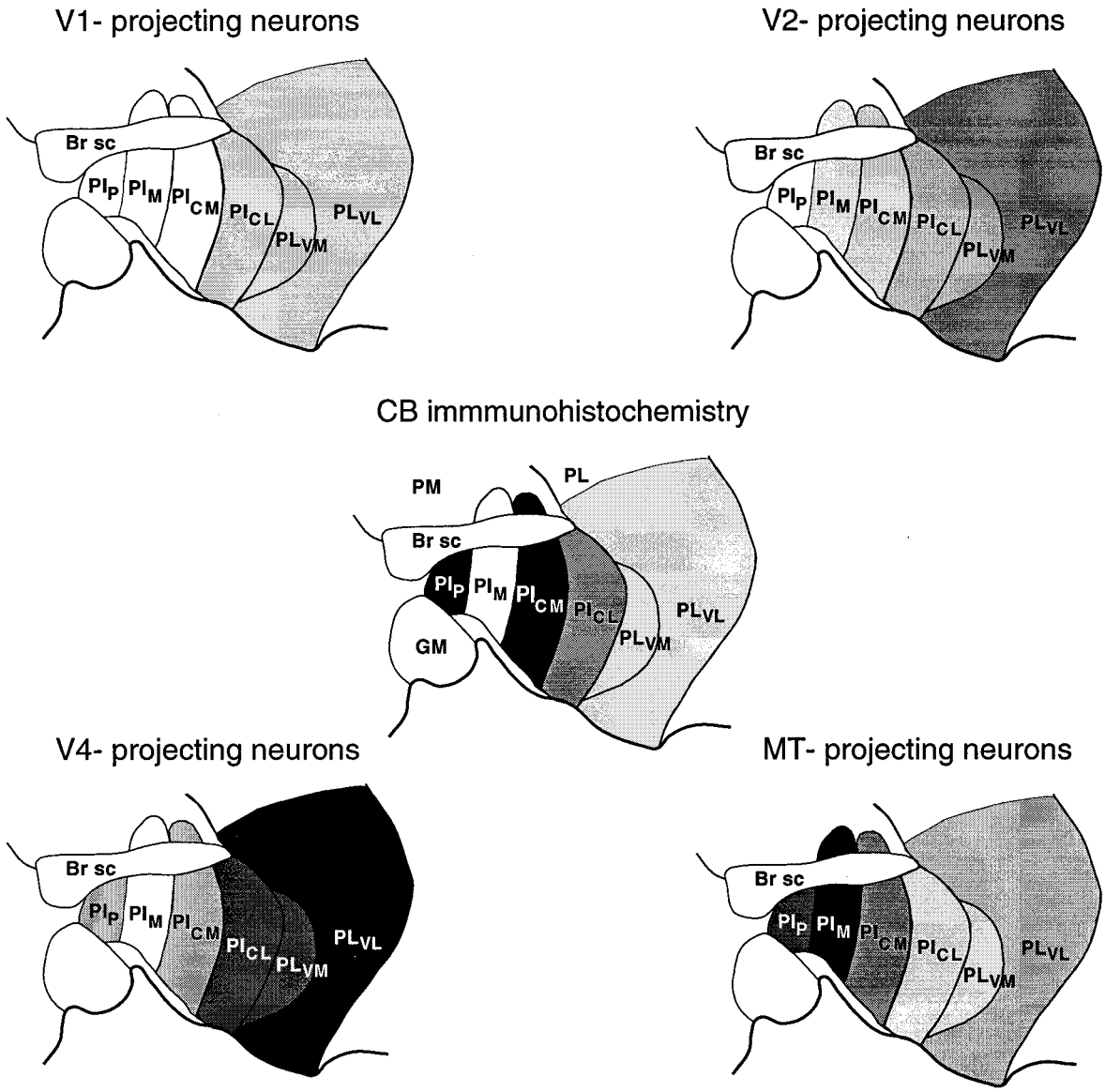

Fig. 9. Schematic showing the subdivisions of the pulvinar based on calbindin immunohistochemistry, and their relationship to connections with areas V1, V2, V4, and MT. The different shades of gray in the center panel represent the different densities of calbindin-positive neurons. The different shades of gray in the surrounding panels indicate the density of retrogradely labeled cells in the different chemoarchitectonic subdivisions of the pulvinar after injections into V1, V2, V4, and MT. For all other conventions, see Figure 5.

retrogradely labeled cells from PI_{CM} to areas V2 and V4. In all of the monkeys with injections in areas MT and V4, there was a clear interdigitation of retrogradely labeled neurons, such that the strongest labeling in P_3 after an MT injection was seen in PI_M, whereas the strongest labeling after a V4 injection was seen in PI_P and PI_{CM} (Figs. 7, 8). Figure 9 summarizes the density of projections from the pulvinar to areas V1, V2, V4, and MT in relation to the subdivisions of the pulvinar based on calbindin immunohistochemistry.

DISCUSSION

The present study confirms early reports that calbindin immunohistochemistry in the pulvinar can be used to further delineate the original cytoarchitectonic subdivisions as described by Olszewski (1952). Both PL and PM were easily distinguished by calbindin immunohistochemistry. In PL, there were both large and small calbindin-containing neurons, as well as horizontally oriented fiber bundles that crossed the area. The PM subdivision, which had both large and small neurons that contained calbindin and intensely stained neuropil, was found dorsomedially to PL. Unlike PL and PM, cytoarchitectonic PI was not a homogenous region. It could be subdivided into PI_P, PI_M, PI_{CM}, and PI_{CL} based on the pattern of calbindin staining. Both the PI_P and PI_{CM} zones displayed the heaviest calbindin immunoreactivity. The PI_{CL} zone had moderate calbindin staining, and PI_M, the "calbindin-hole" zone,

was almost devoid of calbindin immunoreactivity. This pattern of calbindin staining was similar to those described by Stepniewska and Kaas (1997) and Cusick and colleagues (Cusick et al., 1993; Gutierrez et al., 1995).

Functional fields in the pulvinar have been demonstrated based on electrophysiological mapping experiments and connectional studies. As previously described by Bender (1981) and Ungerleider et al. (1984), the P_1 field is found mainly in rostrolateral PI, and extends into portions of adjacent ventromedial PL. The P_2 field, which partially surrounds P_1, is located entirely in ventrolateral PL, and the P_3 field is found in posteromedial PI, but also includes small portions of PL and PM that lie dorsal to the brachium of the superior colliculus. Based on the patterns of calbindin immunohistochemistry, P_1 includes both PI_{CL} and the ventromedial portion of PL, P_2 is located in the ventrolateral portion of PL, and P_3 includes the PI_P, PI_M, and PI_{CM} subdivisions of PI. Based on calbindin immunohistochemistry, it seems that the portions of P_3 that lies above the brachium of the superior colliculus are extensions of PI_M and PI_{CM}. Thus, we used the pattern of calbindin to delineate the dorsal border of P_3.

The subdivisions of the pulvinar are differentially connected with the visual cortex. The neurons projecting to area V1 were found almost exclusively in the PI_{CL} portion of P_1; however, in some cases, the projection also arose from the adjacent ventrolateral subdivision of P_1, located in ventromedial PL. In addition, retrogradely labeled neurons projecting to area V1 were found in P_2, but the projection from P_2 was less dense than that from P_1. The neurons projecting to area V2 were observed to overlap those projecting to area V1 in the same parts of P_1 and P_2. The projection zones to areas V1 and V2 were more widely distributed in P_2 than P_1, which is most likely due the enlarged visual field representation in P_2 relative to P_1. A few double-labeled neurons in P_2 were observed to project to areas V1 and V2. There was an additional projection to area V2 from P_3. In all cases, this projection was found to arise from PI_{CM}, and in some cases there was an additional projection from PI_M; in no case was a projection observed from PI_P to V2.

The neurons projecting to areas V4 and MT were more abundant in the pulvinar than those projecting to areas V1 and V2. In all monkeys, retrogradely labeled neurons projecting to area V4 were observed in both P_1 and P_2, and in PI_{CM} and PI_P of P_3; no cells were found in PI_M. The neurons projecting to area MT were found in P_1 to P_3, with the heaviest projection arising from P_3. Within P_3, the densest projection arose from PI_M. This dense projection from PI_M is similar to the dense projections that were described in previous connectional studies of MT (Standage and Benevento, 1983; Ungerleider et al., 1984; Cusick et al., 1993, Stepniewska et al., 1999). Unlike the neurons projecting to V1 and V2, which largely overlapped, those projecting to MT and V4 were mainly interdigitated, such that the densest projection to MT arose from PI_M and the densest projection to V4 arose from PI_P and PI_{CM}. Connections between V4 and the portions of PI corresponding to PI_P and PI_{CM} have been observed previously (Benevento and Rezak, 1976; Benevento and Davis, 1977; Cusick et al., 1993). A few double-labeled neurons were found to project to areas V4 and MT; they were located in PI_{CL} of P_1 and PI_{CM} of P_3. No double-labeled neurons were found to project to areas V2 and V4 or to areas V2 and MT, even though there were dense overlapping zones in P_1 and P_2 that projected to areas V2 and V4.

Our conclusions on anatomic connections are derived from injections in area V1 in five cases, V2 in seven cases, V4 in six cases, and MT in six cases. However, it should be noted that in all MT cases, there was probable involvement of area FST. The projection from the pulvinar to FST is largely the same as that to MT, but the former is more widespread than the latter, in that it also overlaps the distribution of labeled cells that has been reported after injections of retrograde tracers into parietal visual areas (Asanuma et al., 1985; Boussaoud et al., 1992; Baizer et al., 1993). That is, the projection to FST not only includes P_3 but also regions farther dorsally and caudally in PM that are not connected with MT. Thus, the population of labeled cells we observed in PM beyond the P_3 field likely arose from the inclusion of a small part of FST in the MT injection sites. These cells were not considered in the current analysis. It is of course possible that some of the labeled cells within P_3 projected to FST rather than to MT.

Our subdivisions of the pulvinar based on calbindin immunohistochemistry are similar to those described by Stepniewska and Kaas (1997), but they differ somewhat from those described by Cusick and colleagues (Cusick et al., 1993; Gutierrez et al., 1995). By using a variety of neurochemical markers, including calbindin, the latter authors redefined cytoarchitectonic PI and PL. They divided PI into four distinct regions, PI_P, PI_M, PI_C, and PI_L. Their PI_L extended laterally to include the ventral portion of cytoarchitectonic PL. Thus, the ventral portion of cytoarchitectonic PL was renamed PI_L and $PI_{L\text{-}S}$, or the lateral shell of PI_L. The authors extended PI_L into ventral PL on the basis of immunohistochemistry and connectivity. First, they argued that PI_{CL} and ventral PL are similar neurochemically, except for the appearance of the horizontally oriented fiber bundles in ventral PL. Second, they argued that connectional studies have demonstrated that ventral PL receives input from visual areas of the ventral processing stream whereas dorsal PL receives input from visual areas of the dorsal processing stream. Therefore, they claimed that a dorsal and ventral distinction within the pulvinar has anatomic support. An additional study by Gutierrez and Cusick (1997) demonstrated that area V1 projects to all of the chemoarchitectonic subdivisions of the ventral pulvinar, which they argued supports the idea of the ventral pulvinar being one region, i.e., PI, containing many subdivisions.

Based on the connectional data from our own study and previously published work, we would argue that ventral PL should not be included as part of the inferior pulvinar. Although it may be true that PI_{CL} and ventral PL look similar neurochemically, the connectivity does not support a dorsal/ventral distinction within the pulvinar. First, as noted by Gutierrez et al. (1995), area MT, a key component of the dorsal stream, is connected with the ventral portion of the pulvinar, including P_1, P_2, and P_3 (Ungerleider et al., 1984). Additionally, although the connections of dorsal stream areas FST and MST are mainly with PM, the connections extend ventrally into the P_3 field within PI (Boussaoud et al., 1992). Moreover, V1 and V2 are part of both the dorsal and ventral processing streams, and yet their connections with the pulvinar are limited to its ventral portion (Benevento and Rezak, 1976; Ogren and Hendrickson, 1976; Benevento and Davis, 1977; Rezak and Benevento 1979; Ungerleider et al., 1983; Gutierrez and Cusick, 1997). Finally, the argument that ventral PL should be considered part of PI because V1 projects to all

parts of the inferior pulvinar and ventral PL is unconvincing. This argument does not take into account the separate visual fields maps within PI and PL, in particular, P_1 and P_2. It is clear from our data that ventral PL does project to area V1, but this projection is from a different map, namely, P_2, which is separate from P_1, and which also projects to V1. Accordingly, we have retained the original border between cytoarchitectonic PI and PL.

Our present results indicate that different subdivisions of the pulvinar project preferentially to different visual areas in the cortex. For example, PI_{CM} and PI_P have heavy projections to area V4, whereas PI_M has none and instead projects most heavily to area MT. In addition, within these subdivisions there are differential distributions of calbindin. In PI_{CM} and PI_P, the calbindin immunoreactivity is very dense; however, in PI_M the calbindin staining is sparse. It is possible, therefore, that each of these subdivisions of P_3 contains a separate representation of the visual field. In the cortex, calbindin is observed primarily in a subset of inhibitory GABAergic nonpyramidal neurons but is also seen in pyramidal cells which are non-GABAergic (Baimbridge et al., 1992; Andressen et al., 1993; DeFelipe, 1997; Hof et al., 1999). Calcium-binding proteins are thought to buffer cellular amounts of calcium, which then modulates the signaling within the cell and alters cellular activity (Andressen et al., 1993). Although the functional role of calbindin immunoreactive neurons that are in the thalamus is unknown, these neurons may be involved in modulating activity in the cortex (Jones and Hendry, 1989; Hashikawa et al., 1991). Several studies have shown that the pulvinar is involved in the control of eye movements, the selection of salient stimuli, and the modulation of attention, suggesting that the pulvinar may act to gate incoming information to the cortex (Ungerleider and Christensen, 1977, 1979; Desimone et al., 1990; LaBerge and Buchsbaum, 1990; Robinson and Petersen, 1992). The pattern of retrogradely labeled neurons located within areas of the pulvinar that have differential distributions of calbindin suggests that this protein might serve as one of the modulators of activity in the cortex and may represent a biological substrate for the functional role of the pulvinar. A double-labeling study that would examine the neurochemical profile of these retrogradely labeled neurons needs to be done to assess whether or not these neurons colocalize with calbindin. In addition, the exact role of these calbindin-immunoreactive neurons in visual function remains to be determined.

ACKNOWLEDGMENTS

We thank M. Peralta, III, W.G.M. Janssen, A.P. Leonard, M. Rogell, J.N. Sewell, III, J. Lawrence, and T.W. Galkin for expert technical assistance, and Dr. J.H. Morrison for constant interest and support. P.R.H. received support from the American Health Assistance Foundation and the Brookdale Foundation. R.G. received support from Pronex, CNPq, FAPERJ.

LITERATURE CITED

Adams MM, Webster MJ, Gattass R, Hof PR, Ungerleider LG. 1995. Inputs to visual areas V1, V2, MT from the macaque pulvinar and their relationships to chemoarchitectonic subdivisions. Soc Neurosci Abstr 21:904.

Andressen C, Blümcke I, Celio MR. 1993. Calcium-binding proteins: selective monkey markers of nerve cells. Cell Tissue Res 271:181–208.

Asanuma C, Andersen RA, Cowan WM. 1985. The thalamic relations of the caudal inferior parietal lobule and the lateral prefrontal cortex in monkeys: divergent cortical projections from cell clusters in the medial pulvinar nucleus. J Comp Neurol 241:357–381.

Baimbridge KG, Celio MR, Rogers JH. 1992. Calcium-binding proteins in the nervous system. Trends Neurosci 15:303–308.

Baizer JS, Desimone R, Ungerleider LG. 1993. Comparison of subcortical connections of inferior temporal and posterior parietal cortex in monkeys. Vis Neurosci 10:59–72.

Bender DB. 1981. Retinotopic organization of macaque pulvinar. J Neurophysiol 46:672–693.

Benevento LA, Davis B. 1977. Topographical projections of the prestriate cortex to the pulvinar nuclei in the macaque monkey: an autoradiographic study. Exp Brain Res 30:405–424.

Benevento LA, Fallon JH. 1975. The ascending projections of the superior colliculus in the rhesus monkey (*Macaca mulatta*). J Comp Neurol 160:339–362.

Benevento LA, Rezak M. 1976. The cortical projections of the inferior pulvinar and adjacent lateral pulvinar in the rhesus monkey (*Macaca mulatta*): an autoradiographic study. Brain Res 108:1–24.

Boussaoud D, Ungerleider LG, Desimone R. 1990 Pathways for motion analysis: cortical connections of the medial superior temporal and fundus of the superior temporal visual areas in the macaque. J Comp Neurol 296:462–495.

Boussaoud D, Desimone R, Ungerleider LG. 1992. Subcortical connections of visual areas MST and FST in macaques. Vis Neurosci 9:291–302.

Campbell MJ, Hof PR, Morrison JH. 1991. A subpopulation of primate corticocortical neurons is distinguished by somatodendritic distribution of neurofilament protein. Brain Res 539:133–136.

Campos-Ortega JA, Hayhow WR. 1972. On the organization of the visual cortical projection to the pulvinar in the *Macaca mulatta*. Brain Behav Evol 6:394–423.

Celio MR, Baier W, Gregersen HG, De Viragh PA, Schärer L, Norman AW. 1990. Monoclonal antibodies directed against the calcium-binding protein calbindin D-28k. Cell Calcium 11:599–602.

Chalupa LM. 1991. The visual function of the pulvinar. In: Leventhal AG, editor. The neural basis of visual function. London: Macmillan. p 140–159.

Cusick CG, Kaas JH. 1988 Cortical connections of area 18 and dorsolateral visual cortex in squirrel monkeys. Vis Neurosci 1:211–237.

Cusick CG, Scripter JL, Darensberg JG, Weber JT. 1993. Chemoarchitectonic subdivisions of the visual pulvinar in monkeys and their connectional relations with the middle temporal and rostral dorsolateral visual areas, MT and DLr. J Comp Neurol 336:1–30.

Daniel PM, Whitteridge D. 1961. The representation of the visual field on the cerebral cortex in monkeys. J Physiol (Lond) 159:203–221.

DeFelipe J. 1997. Types of neurons, synaptic connections and chemical characteristics of cells immunoreactive for calbindin-D28K, parvalbumin and calretinin in the neocortex. J Chem Neuroanat 14:1–19.

Desimone R, Ungerleider LG. 1986. Multiple visual areas in the caudal superior temporal sulcus of the macaque. J Comp Neurol 248:164–189.

Desimone R, Wessinger M, Thomas L, Schneider W. 1990. Attentional control of visual perception: cortical and subcortical mechanisms. Cold Spring Harb Symp Quant Biol 55:963–971.

Gattass R, Gross CG. 1981. Visual topography of striate projection zone (MT) in posterior superior temporal sulcus of the macaque. J Neurophysiol 46:621–638.

Gattass R, Gross CG, Sandell JH. 1981. Visual topography of V2 in the macaque. J Comp Neurol 201:519–539.

Gattass R, Sousa APB, Gross CG. 1988. Visuotopic organization and extent of V3 and V4 of the macaque. J Neurosci 8:1831–1845.

Graham J. 1982. Some topographical connections of the striate cortex with subcortical structures in *Macaca fascicularis*. Exp Brain Res 47:1–14.

Gray D, Gutierrez C, Cusick CG. 1999 Neurochemical organization of inferior pulvinar complex in squirrel monkeys and macaques revealed by acetylcholinesterase histochemistry, calbindin and CAT-301 immunostaining, and *Wisteria floribunda* agglutinin binding. J Comp Neurol 409:452–468.

Gutierrez C, Cusick CG. 1997. Area V1 in macaque monkeys projects to multiple histochemically defined subdivisions of the inferior pulvinar complex. Brain Res 765:349–356.

Gutierrez C, Yaun A, Cusick CG. 1995. Neurochemical subdivisions of the inferior pulvinar in macaque monkeys. J Comp Neurol 363:545–562.

Harting JK, Huerta MF, Frankfurter AJ, Strominger NL, Royle GJ. 1980.

Ascending pathways from the monkey superior colliculus: an autoradiographic study. J Comp Neurol 192:853–882.

Hashikawa T, Rausell E, Molinari M, Jones EG. 1991. Parvalbumin- and calbindin-containing neurons in the monkey medial geniculate complex differential distribution and cortical layer specific projections. Brain Res 544:335–341.

Hof PR, Morrison JH. 1995. Neurofilament protein defines regional patterns of cortical organization in the macaque monkey visual system: a quantitative immunohistochemical analysis. J Comp Neurol 352:161–186.

Hof PR, Nimchinsky EA. 1992. Regional distribution of neurofilament and calcium-binding proteins in the cingulate cortex of the macaque monkey. Cereb Cortex 2:456–467.

Hof PR, Nimchinsky EA, Morrison JH. 1995. Neurochemical phenotype of corticocortical connections in the macaque monkey: quantitative analysis of a subset of neurofilament protein-immunoreactive projection neurons in frontal, parietal, temporal, cingulate cortices. J Comp Neurol 362:109–133.

Hof PR, Glezer II, Condé F, Flagg RA, Rubin MB, Nimchinsky EA, Vogt Weisenhorn DM. 1999. Cellular distribution of the calcium-binding proteins parvalbumin, calbindin, calretinin in the neocortex of mammals: phylogenetic and developmental patterns. J Chem Neuroanat 16:77–116.

Jones EG. 1985. The thalamus. New York: Plenum Press.

Jones EG, Hendry SHC. 1989. Differential calcium binding protein immunoreactivity distinguishes classes of relay neurons in monkey thalamic nuclei. Eur J Neurosci 1:222–246.

LaBerge D, Buchsbaum MS. 1990. Positron emission tomography measurements of pulvinar activity during an attention task. J Neurosci 10:613–619.

Maunsell JHR, Van Essen DC. 1983. The connections of the middle temporal visual area (MT) and their relationship to a cortical hierarchy in the macaque monkey. J Neurosci 3:2563–2586.

Ogren MP, Hendrickson AE. 1976. Pathways between striate cortex and subcortical regions in *Macaca mulatta* and *Saimiri sciureus*: evidence for a reciprocal pulvinar connection. Exp Neurol 53:780–800.

Olszewski J. 1952. The thalamus of the *Macaca mulatta*, an atlas for use with the stereotaxic instrument. Basel: Karger.

Partlow GD, Colonnier M, Szabo J. 1977. Thalamic projections of the superior colliculus in the rhesus monkey, *Macaca mulatta*: a light and electron microscopic study. J Comp Neurol 171:285–318.

Petersen SP, Robinson DL, Keys W. 1985. Pulvinar nuclei of the behaving rhesus monkey: visual responses and their modulation. J Neurophysiol 54:867–886.

Rausell E, Jones EG. 1991. Histochemical and immunocytochemical compartments of the thalamic VPM nucleus in monkeys and their relationship to the representational map. J Neurosci 11:210–225.

Rezak M, Benevento LA. 1979. A comparison of the organization of the projections of the dorsal lateral geniculate nucleus, the inferior pulvinar and the adjacent lateral pulvinar to primary visual cortex (area 17) in the macaque monkey. Brain Res 167:19–40.

Robinson DL, Petersen SE. 1992. The pulvinar and visual salience. Trends Neurosci 15:127–132.

Robinson DL, Petersen SE, Keys W. 1986. Saccade-related and visual activities in the pulvinar nuclei of the behaving rhesus monkey. Exp Brain Res 62:625–634.

Rosene DL, Roy NJ, Davis BJ. 1986. A cryoprotection method that facilitates cutting frozen sections of whole monkey brains for histological and histochemical processing without freezing artifact. J Histochem Cytochem 34:1301–1315.

Standage GP, Benevento LA. 1983. The organization of connections between the pulvinar and visual area MT in the macaque monkey. Brain Res 262:288–294.

Stepniewska I, Kaas JH. 1997. Architectonic subdivisions of the inferior pulvinar in new world and old world monkeys. Vis Neurosci 14:1043–1060.

Stepniewska I, Qi H-X, Kaas JH. 1999 Do superior colliculus projection zones in the inferior pulvinar project to MT in primates? Eur J Neurosci 11:469–480.

Ungerleider LG, Christensen CA. 1977. Pulvinar lesions in monkeys produce abnormal eye movements during visual discrimination training. Brain Res 136:189–96.

Ungerleider LG, Christensen CA. 1979. Pulvinar lesions in monkeys produce abnormal scanning of a complex visual array. Neuropsychologia 17:493–501.

Ungerleider LG, Desimone R. 1986. Cortical connections of the visual area MT in the macaque. J Comp Neurol 248:190–222.

Ungerleider LG, Galkin TW, Mishkin M. 1983. Visuotopic organization of projections from striate cortex to inferior and lateral pulvinar in rhesus monkey. J Comp Neurol 217:137–157.

Ungerleider LG, Mishkin M. 1979. The striate projection zone in the superior temporal sulcus of location and topographic organization. J Comp Neurol 188:347–366.

Ungerleider LG, Desimone R, Galkin TW, Mishkin M. 1984. Subcortical projections of area MT in the macaque. J Comp Neurol 223:368–386.

Van Essen DC, Maunsell JHR, Bixby JL. 1981. The middle temporal visual area in the macaque: myeloarchitecture, connections, functional properties and topographic connections. J Comp Neurol 199:293–326.

Zeki SM. 1974 Functional organization of a visual area in the posterior bank of the superior temporal sulcus of the rhesus monkey. J Physiol (Lond) 236:549–573.